Optimal Search and Interdiction Planning

Jesse Pietz[a], Johannes O. Royset[b]

[a] *United States Air Force Academy, USAF Academy, CO, USA*
[b] *Naval Postgraduate School, Monterey, CA*

The views expressed in this article are those of the authors and do not necessarily reflect the official policy or position of the Air Force, the Department of Defense, or the U.S. Government.

Abstract

International law enforcement organizations around the world endeavor to combat high drug related mortality rates by seizing illicit drugs in transit over international waters. This mission requires effective plans that route multiple aerial searchers and position surface interdictors through large expanses of geographical areas in the presence of highly uncertain estimates about drug smuggler whereabouts. This high uncertainty combined with the challenge of coordinating search and interdiction make it particularly difficult to conduct mission planning. We present optimal search and interdiction models that address these important challenges and demonstrate how planners can used these models by applying them to a realistic counterdrug operation scenario.

Keywords: OR in defense, Optimal search, Search theory, Counterdrug operations

1. Introduction

1.1. Background

We consider the task of a mission planner for a unit charged with searching for and interdicting drug smugglers over international waters. Each day the planner receives intelligence estimates about where and when smugglers may be moving over the next mission execution period. Naturally, there is uncertainty regarding the accuracy of these estimates. A limited number of aerial search and surface interdiction assets can be used. The goal is to develop a mission plan for the mission execution period that utilizes these assets as effectively as possible by maximizing the expected amount of drugs interdicted.

Scenarios like this are faced by many organizations around the world in order to combat the effects of an alarmingly high drug related mortality rate. Approximately 1 in every 100 adult deaths world wide can attributed to illicit drug use (United Nations Office on Drugs and Crime, 2012, p. 1) and over 1,500 metric tons of illegal drugs are seized in transit to United States annually (US

Report Documentation Page

Form Approved
OMB No. 0704-0188

1. REPORT DATE	2. REPORT TYPE	3. DATES COVERED
18 JUN 2014		**00-00-2014 to 00-00-2014**

4. TITLE AND SUBTITLE	5a. CONTRACT NUMBER
Optimal Search and Interdiction Planning	5b. GRANT NUMBER
	5c. PROGRAM ELEMENT NUMBER
6. AUTHOR(S)	5d. PROJECT NUMBER
	5e. TASK NUMBER
	5f. WORK UNIT NUMBER
7. PERFORMING ORGANIZATION NAME(S) AND ADDRESS(ES) **Naval Postgraduate School,Monterey,CA,93943**	8. PERFORMING ORGANIZATION REPORT NUMBER
9. SPONSORING/MONITORING AGENCY NAME(S) AND ADDRESS(ES)	10. SPONSOR/MONITOR'S ACRONYM(S)
	11. SPONSOR/MONITOR'S REPORT NUMBER(S)

12. DISTRIBUTION/AVAILABILITY STATEMENT
Approved for public release; distribution unlimited

13. SUPPLEMENTARY NOTES

14. ABSTRACT

International law enforcement organizations around the world endeavor to combat high drug related mortality rates by seizing illicit drugs in transit over international waters. This mission requires e ective plans that route multiple aerial searchers and position surface interdictors through large expanses of geographical areas in the presence of highly uncertain estimates about drug smuggler whereabouts. This high uncertainty combined with the challenge of coordinating search and interdiction make it particularly di cult to conduct mission planning. We present optimal search and interdiction models that address these important challenges and demonstrate how planners can used these models by applying them to a realistic counterdrug operation scenario.

15. SUBJECT TERMS

16. SECURITY CLASSIFICATION OF:			17. LIMITATION OF ABSTRACT	18. NUMBER OF PAGES	19a. NAME OF RESPONSIBLE PERSON
a. REPORT **unclassified**	b. ABSTRACT **unclassified**	c. THIS PAGE **unclassified**	**Same as Report (SAR)**	**25**	

Department of Justice, 2014). One such organization that strives to combat this problem is the Joint Interagency Task Force South (JIATF-S). JIATF-S conducts detection and monitoring operations, and facilitates the interdiction of illicit trafficking in the waters surrounding South and Central America (Joint Interagency Task Force South, 2014). Complicating the task of mission planning for multiple assets in the face of uncertain intelligence estimates about smuggler whereabouts is the fact that the geographical Area of Interest (AOI) to be covered may be quite large; 42-million square miles in the case of JIATF-S (Munsing and Lamb, 2011).

Returning to the task of the mission planner, it is unclear how to capitalize on the intelligence about smugglers by routing aerial searchers and positioning surface interdictors within such a large AOI. In the absence of sophisticated techniques one may be tempted to direct assets to the most valuable smugglers, where value may be associated with their expected payload. This manual approach has been shown to result in suboptimal search plans because it fails to balance the limitations of available assets with the transit requirements that are necessary in a large AOI (Pietz and Royset, 2013).

1.2. Related Work

Much attention has been paid in the literature to the topic of optimal search. Path-constrained optimal search problems are concerned with determining the best routing for searchers in order to detect targets in some defined AOI. Path-constrained optimal search problems are known to be NP-hard (Trummel and Weisinger, 1986). Benkoski et al. (1991) summarize much of the search theory literature through 1991. Recent research in optimal search has focused on discrete-time and -space models, developing various techniques to reduce solution times such as specialized branch-and-bound algorithms (see, e.g., Stewart 1979, Eagle and Yee 1990, Dell et al. 1996, Sato and Royset 2010), heuristics (see, e.g., Dell et al. 1996, Grundel 2005, Wong et al. 2005), and cutting-plane approaches (see, e.g., Royset and Sato 2010). Optimal search problem formulations have become more versatile in their ability to account for multiple cooperating searchers, multiple targets with different characteristics, as well as environmental effects on the search (see, e.g., Dell et al. 1996, Wong et al. 2005, Riehl et al. 2007, Royset and Sato 2010). In contrast to these models, Pietz and Royset (2013) present a continuous-time and -space optimal search model called the Smuggler Search Problem (SSP), which is solved by a branch-and-bound algorithm. None of these models, however, deal with the problem of interdictor positioning.

Coordinating search plans with interdiction assets is an important real-world consideration. Few

studies in the literature focus on this aspect of mission planning. Kress et al. (2012) examine a discrete-time and -space stochastic Dynamic Programming (DP) approach to coordinate the efforts of a single aerial search asset and a single surface interdiction asset. This model can, in principle, be solved by a backward DP algorithm, but becomes intractable when one considers problems arising from real-world scenarios. Accordingly, a greedy heuristic is proposed to obtain solutions. Related work has been done in studying search and action problems (see Sun 2009, Jin et al. 2006), however these models consider multi-role aerial assets with some combination of sensing, intercept, and attack capabilities. Supporting the mission of organizations like JIATF-S requires the development of a new approach to modeling coordinated search and interdiction operations that leads to problems which are solvable for real-world scenarios.

1.3. Organization

The remainder of this paper is organized as follows. Next we describe a hypothetical mission planning scenario that is representative of real-world counterdrug operations and illustrate where current modeling falls short in capturing all the necessary planning considerations. In Sections 3 and 4, we proceed to develop two extensions to the SSP that address these modeling shortfalls and illustrate their use with our benchmark scenario. We conclude with final remarks in Section 5.

2. Benchmark Scenario and Modeling Limitations

2.1. Scenario Definition

In order to motivate the search model enhancements that will be presented shortly, we define a benchmark mission planning scenario. Researchers and practitioners developed this scenario, using unclassified open source data, so that it is representative of the real-world issues faced by planners. Our benchmark scenario (**BS**) involves four targets (smugglers), two aerial searchers, and three surface interdiction assets. Intelligence assessmets provide the departure time as well as the departure, arrival, and path waypoint locations of each target, but these data are uncertain. The accuracy of the intelligence results in additional uncertainty as there is a chance that the intelligence is completely wrong and the target is not present. Figure 1 depicts a spatial representation of the expected, based on intelligence assessments, movement tracks for these targets.

There are two P-3 search aircraft available for planning, each operating out of Comalapa Airbase, El Salvador. The aircraft have a maximum cruise speed (V) of 325 kts, an on-station speed ($\hat{V}$) of 205 kts, and a 10-h endurance (T). In order to account for maintenance and aircrew rest periods,

Figure 1: **Baseline scenario BS** - Spatial representation of expected target tracks in the baseline scenario. The searchers' home station is identified by "×". Four total targets transiting the AOI during the one-day mission execution period. Timing and uncertainty of target tracks not shown.

we assume that each aircraft can execute no more than a single search sortie during the 24-h mission execution period D.

Throughout this scenario, there are three surface ships available for interdiction support as needed. Two can be positioned anywhere in the eastern Pacific Ocean and the other one can be positioned anywhere in the Caribbean Sea. Each has an intercept speed (V_I) of 20 kts. Surface interdictors are to be positioned in coordination with the search plan so that they are able to respond if a searcher detects a target. When a target is detected by a searcher, the searcher monitors the target and summons an interdictor. The interdictor must then transit from its standby location to the location where the target is being monitored. A successful interdiction occurs once the interdictor arrives. Due to high cost of repositioning surface assets, we assume that interdictors cannot be routed and that they will remain in their stand-by position until called upon to respond when a detection occurs.

While there is uncertainty with regard to where and when each target departs, where the target arrives, and the value of interdicting the target, the nature of the intelligence allows the mission planner to estimate these values within some range of uncertainty. These assessed target data, listed in Table 1, form a moving box (*search region*) for each target within which search may be conducted.

Number of targets	n
Speed of target j	U_j
Expected departure time of target j	τ_j
Time uncertainty range of target j	$\tilde{\tau}_j$
Expected departure location of target j	$\boldsymbol{\rho}_j$
Expected arrival location of target j	$\bar{\boldsymbol{\rho}}_j$
Departure/arrival location uncertainty range of target j	$\tilde{\rho}_j$
Expected value of detecting target j	q_j

Table 1: **Assessed target data**

The first target (GF1) is a GO FAST boat that is expected to be carrying 1,000 kg of drugs and traveling in the Caribbean at an expected speed (U_1) of 50 kts. A GO FAST boat is a large speed boat that is often outfitted with additional engines at the stern. These boats are commonly used by maritime smugglers. The expected track of GF1 is a coastal route that transits through the longitude/latitude points: 76.3W 9N - 79W 10N - 82W 10N - 83.5W 14N. The location of departure (76.3W 9N) and the arrival location (83.5W 14N) both have a uniform uncertainty range of ±30 nm. There is a 60 nm × 60 nm uniform range of uncertainty about each waypoint (79W 10N, 82W 10N). GF1 is expected to depart at time 0000 with uniform departure time uncertainty of ±2 h. There is a 0.95 probability that the intelligence about GF1 is correct. For brevity we call this probability the *intelligence certainty* about GF1. The expected detection value (q_1) of GF1 is the product of the payload and the intelligence certainty $q_1 = 1,000 \times 0.95 = 950$ kg. The sweep width W of a P-3 against a GO FAST boat is assumed to be 15 nm.

The second target (GF2) is a GO FAST boat that is expected to be carrying 1,500 kg of drugs and traveling in the Caribbean at an expected speed (U_3) of 50 kts. The expected track of GF2 is a straight-line route that transits through the longitude/latitude points: 72W 12N - 87.5W 20N. The location of departure (72W 12N) and the arrival location (87.5W 20N) both have a uniform uncertainty range of ±30 nm. GF2 is expected to depart at time 2400, which is on the day after the mission execution period, however it has a uniform departure time uncertainty of ±24 h that makes it possible that GF2 is on the water sometime during the mission execution period. The intelligence certainty about GF2 is 0.50, thus the expected detection value (q_3) of GF2 is the product of the payload and the intelligence certainty $q_3 = 1,500 \times 0.50 = 750$ kg.

The third target (SP1) is a Self-Propelled Semi-Submersible vessel (SPSS) that is expected to

be carrying 2,500 kg of drugs and traveling in the eastern Pacific at an expected speed (U_7) of 15 kts. An SPSS is a low profile smuggler vessel that keeps most of its structure under water. The expected track of SP1 is an angled route that transits through the longitude/latitude points: 77W 5N - 86W 3N - 92.2W 14.5N. The location of departure (77W 5N) and the arrival location (92.2W 14.5N) both have a uniform uncertainty range of ±40 nm. SP1 is expected to depart at time 0500 with uniform departure time uncertainty of ±3 h. The intelligence certainty about SP1 is 0.50, thus the expected detection value (q_7) of SP1 is the product of the payload and the intelligence certainty $q_7 = 2,500 \times 0.50 = 1,250$ kg. Due to the low profile of an SPSS, the sweep width W of a P-3 against this type of vessel is assumed to be 5 nm.

The fourth target (GF3) is a GO FAST boat that is expected to be carrying 2,000 kg of drugs and traveling in the eastern Pacific at an expected speed (U_9) of 50 kts. The expected track of GF3 is an angled route that transits through the longitude/latitude points: 79W 1N - 92W 2S - 94W 16N. The location of departure (79W 1N) has a uniform uncertainty range of ±25 nm. The arrival location (94W 16N) has a uniform uncertainty range of ±50 nm. There is also a 50 nm × 50 nm uniform range of uncertainty about the waypoint (92W 2S). GF3 is expected to depart at time 0500 with uniform departure time uncertainty of ±2 h. The intelligence certainty about GF3 is 0.95, thus the expected detection value (q_9) of GF3 is the product of the payload and the intelligence certainty $q_9 = 2,000 \times 0.95 = 1,900$ kg. By virtue of its large expected detection value and its relatively narrow uncertainty range, GF3 is considered a high-value target in this scenario.

In a four-target scenario, developing a mission plan, even for a single searcher, is not an easy task for a planner. Varying target speeds and payloads, differing levels of certainty, and timing constraints during the execution period present many challenges. Clearly, since **BS** is more complex, developing a good plan manually would be an even harder task for a mission planner.

2.2. The Smuggler Search Problem

In this section we review the SSP presented in Pietz and Royset (2013) in order to form a basis for model extensions discussed later. The SSP is an optimal search model defined on a directed network $G = (N, A)$ of linearly moving search regions that each contain a target. Using the property of linear motion, the latest departure time τ_j^{min} and the earliest arrival time τ_j^{max} can easily be calculated for each target j. We assume random search within each search region and define the searcher's detection rate α_j against each target j as a ratio of the searcher's sweep width W and its on-station speed $\hat{V}$ to the area of the search region $\tilde{\tau}_j \tilde{\rho}_j U_j$ (Washburn 2002, ch. 2). We arrive at the following

optmial search mixed-integer nonlinear programming formulation.

Problem SSP:

$$\max_{\boldsymbol{a},\boldsymbol{d},\boldsymbol{t},\boldsymbol{x},\boldsymbol{y}} \quad \sum_{j\in\hat{N}} q_j \left(1-\exp\left\{-\alpha_j d_j y_j\right\}\right) \tag{1a}$$

$$\text{s.t.} \quad (||\boldsymbol{\rho}_i + (a_i + d_i - \tau_i)\boldsymbol{u}_i - \boldsymbol{\rho}_j$$

$$\ldots - (a_i + d_i + t_{i,j} - \tau_j)\boldsymbol{u}_j||$$

$$\ldots - Vt_{i,j})x_{i,j} \leq 0, \qquad \forall (i,j) \in A \tag{1b}$$

$$(a_i + d_i + t_{i,j} - a_j)\, x_{i,j} \leq 0, \qquad \forall (i,j) \in A \tag{1c}$$

$$\sum_{j\in\hat{N}} d_j + \sum_{(i,j)\in A} t_{i,j} \leq T \tag{1d}$$

$$\sum_{j\in N} d_j + \sum_{(i,j)\in A} t_{i,j} \leq D \tag{1e}$$

$$a_j \geq \tau_j^{min}, \quad \forall j \in N \tag{1f}$$

$$a_j + d_j \leq \tau_j^{max}, \quad \forall j \in N \tag{1g}$$

$$a_0 = 0 \tag{1h}$$

$$d_{n+1} = 0 \tag{1i}$$

$$a_j, d_j \geq 0, \qquad \forall j \in N \tag{1j}$$

$$t_{i,j} \geq 0, \qquad \forall (i,j) \in A \tag{1k}$$

$$\boldsymbol{y} = \boldsymbol{\Gamma}\boldsymbol{x} \tag{1l}$$

$$\boldsymbol{x} \in \mathbb{X} \tag{1m}$$

The objective (1a) is to maximize the expected value of the search effort by choice of the searcher's arrival time a_j at each search region j, its transit time $t_{i,j}$ from search region i to search region j, its search dwell time d_j in search region j, binary visitation variables y_j to each search region j, and binary arc flow variables $x_{i,j}$ from i to j. Vectorized terms are shown in bold font. Constraints (1b) ensure that search region j is reachable from search region i in time $t_{i,j}$ given the searcher's speed V. Constraints (1c) propagate arrival times $\boldsymbol{a}$ forward in time as the search transits from one search region to the next. Constraint (1d) ensures that the total flying hours of the searcher does not exceed its endurance limit T. Similarly, constraint (1e) ensures that the time horizon of the plan

stays within the mission execution period D. Constraints (1f) require that the vehicle be routed to a search region only after the target has surely departed. Similarly, constraints (1g) preclude searching in a region after the target has possibly arrived. Constraint (1h) ensures that the scenario starts at time 0000, while constraint (1i) ensures that the scenario ends when the searcher returns to its home station. Constraints (1j) and (1k) enforce nonnegativity, while constraints (1l) and (1m) capture standard network flow balance and routing subtour elimination constraints. This model is easily extended to account for nonlinear target movement tracks using piecewise linear approximation and multiple searchers by expanding the network G. Problem instances are solved using a specialized branch-and-bound algorithm (SBB), which is designed to solve Generalized Orienteering Problems. All of the models we consider in this paper fall withing this class of problems.

2.3. Modeling Limitations

Returning to our benchmark scenario, we observe that the SSP does not allow us to model GF2 because its large time uncertainty window of ±24 h yields a search region that spans its entire movement track. Furthermore, the model does not consider the positioning of interdiction assets. If we remove GF2 and the interdictors, we are able to compute an optimal search plan for this restricted scenario by solving the SSP using SBB. For brevity, we refer to this restricted scenario as **BS-MS**. We also denote by $\boldsymbol{\theta}_j^+$ and $\boldsymbol{\theta}_j^-$ the respective locations in search region j where the searcher begins and ends search for target j. In this model, $\boldsymbol{\theta}_j^+$ corresponds to the expected location of target j the moment search begins at time a_j, and $\boldsymbol{\theta}_j^-$ corresponds to the expected location of target j the moment search ends at time $a_j + d_j$. The search times and searcher path for the optimal solution are shown in Table 2. Figure 2 shows a spatial representation of the optimal search plan.

The solution to **BS-MS** provides insight to the planner and clearly identifies how to route both searchers. Unfortunately, it does not account for the presence of GF2 in the scenario nor does it tell the planner where to position interdiction assets. The planner must hope that GF2 is not a worthwhile target to search and that he is able to position interdiction assets in order to support this search plan without prior coordination. In the case where it is beneficial to search GF2, this plan is suboptimal. In the case where it is not possible to position interdictors so that they are able to cover all searched areas, then the planner runs the risk that a detected target will get away because an interdictor is unable to intercept it. We now address these issues in turn.

Searcher	Target	t	a	d	$\boldsymbol{\theta}^+$	$\boldsymbol{\theta}^-$
1	Home	-	0	8.40	(89.1W 13.4N)	(89.1W 13.4N)
	GF3	2.68	11.08	4.64	(83.9W 0.1S)	(87.7W 1.0S)
	Home	2.68	18.40	-	(89.1W 13.4N)	(89.1W 13.4N)
2	Home	-	0	6.39	(89.1W 13.4N)	(89.1W 13.4N)
	GF1	1.37	7.76	1.91	(82.2W 10.6N)	(82.8W 12.0N)
	SP1	1.57	11.24	2.69	(78.5W 4.7N)	(79.2W 4.5N)
	Home	2.46	16.39	-	(89.1W 13.4N)	(89.1W 13.4N)

Table 2: **Optimal search times and searcher path for scenario BS-MS** - Searcher 1 is routed to search GF3 for just over 4.5 h. Searcher 2 is routed to search GF1 for nearly 2 h, then moves on to search SP1 for just over 2.5 h. The remainder of each searcher's 10-h endurance is spent in transit. The expected value of the search plan is 2,254.6 kg of drugs detected.

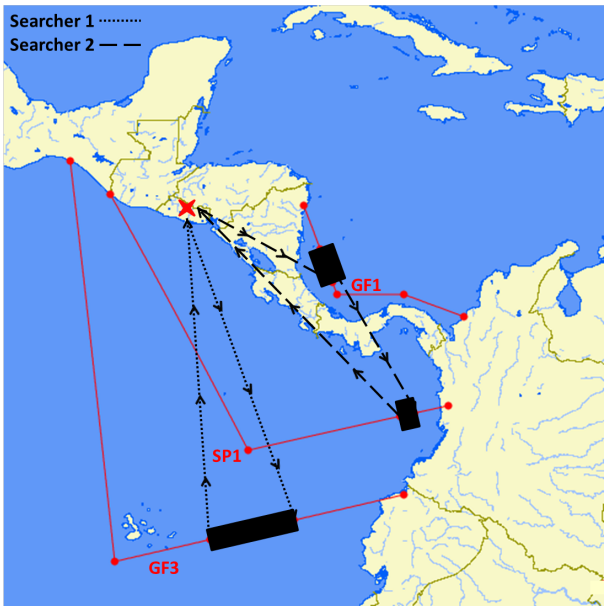

Figure 2: **Scenario BS-MS solution** - Spatial representation of **BS-MS** optimal solution. Searcher 1 is routed to search GF3. Searcher 2 is routed to search GF1 and then moves on to search SP1. Each rectangular block represents a moving search region and its size corresponds to the total area of the search region during the time when the searcher is performing search actions. Arrows indicate the direction of each searcher's path.

3. Highly Uncertain Assessed Target Data

3.1. Fixed Region Search Model

Suppose that the uncertainty associated with a target track is such that using a moving search region is not realistic. This can happen, for example, when the departure time uncertainty range is

large or when there is unpredictable variation in the target speed. In this case, we model the search for targets using a random search model (Washburn 2002, ch. 2) applied to a static *fixed region*.

In a sense a fixed-region model is less complex than that of the SSP which considers moving search regions. However, a subtle practical matter must be considered. The SSP implicitly assumes that the moving search regions are not too large. As such, the question of where within the search region a searcher is routed to and from is insignificant. Travel distances are calculated by routing the searcher through the center of each search region that is assigned. When the search region is small, the chosen tactical search pattern can be accommodated with a negligible difference in the searcher's entry and exit locations in this region. In the situation when the search region is large, we must account for the difference in entry and exit points. We do this by including the entry and exit locations in the model as decision variables.

We model searcher transit to and from a convex subset $\mathcal{R}_j$ of the fixed region associated with target j. We denote by $\boldsymbol{r}_j^+$ and $\boldsymbol{r}_j^-$ the respective entry and exit location of the searcher in fixed region j. We model both moving and fixed regions by introducing the respective disjoint subsets Q and R, where $Q \cup R = N$ are the nodes in the directed network G. We include the home station and recovery location in the set Q. It is convenient to define $\hat{Q} = Q \backslash \{0, n+1\}$. Directed arcs are defined between all $(i, j) \in A$ as follows. Let A_{QQ} be the set of arcs connecting a moving search region to another moving search region. Let A_{QR} be the set of arcs connecting a moving search region to fixed search region. A_{QR} and A_{RR} are defined similarly. We introduce the vectorized location notation $\boldsymbol{r}_j = (\boldsymbol{r}_j^+, \boldsymbol{r}_j^-)$, and $\boldsymbol{r} = (\boldsymbol{r}_{j_1}, \boldsymbol{r}_{j_2}, \ldots, \boldsymbol{r}_{j_{|R|}})$. Accounting for fixed region targets, the modified SSP is stated as follows.

Problem SSP-FR:

$$\max_{\boldsymbol{a},\boldsymbol{d},\boldsymbol{t},\boldsymbol{r},\boldsymbol{x},\boldsymbol{y}} \quad \sum_{j\in\hat{N}} q_j\left(1-\exp\left\{-\alpha_j d_j y_j\right\}\right) \tag{2a}$$

$$\text{s.t.} \quad (||\boldsymbol{\rho}_i + (a_i + d_i - \tau_i)\boldsymbol{u}_i - \boldsymbol{\rho}_j \ldots - (a_i + d_i + t_{i,j} - \tau_j)\boldsymbol{u}_j|| \ldots - Vt_{i,j})x_{i,j} \leq 0, \quad \forall (i,j) \in A_{QQ} \tag{2b}$$

$$(||\boldsymbol{\rho}_i + (a_i + d_i - \tau_i)\boldsymbol{u}_i - \boldsymbol{r}_j^+|| \ldots - Vt_{i,j})x_{i,j} \leq 0, \quad \forall (i,j) \in A_{QR} \tag{2c}$$

$$(||\boldsymbol{r}_i^- - \boldsymbol{\rho}_j - (a_i + d_i + t_{i,j} - \tau_j)\boldsymbol{u}_j|| \ldots - Vt_{i,j})x_{i,j} \leq 0, \quad \forall (i,j) \in A_{RQ} \tag{2d}$$

$$(||\boldsymbol{r}_i^- - \boldsymbol{r}_j^+|| - Vt_{i,j})x_{i,j} \leq 0, \quad \forall (i,j) \in A_{RR} \tag{2e}$$

$$(||\boldsymbol{r}_j^- - \boldsymbol{r}_j^+|| - \hat{V}d_j)y_j \leq 0, \quad \forall j \in R \tag{2f}$$

$$\boldsymbol{r}_j^-, \boldsymbol{r}_j^+ \in \mathcal{R}_j, \quad \forall j \in R \tag{2g}$$

$$\text{(1c) – (1m)}$$

Constraints (2b) through (2e) ensure that the time it takes the searcher to travel between each pair of regions, moving or fixed, is feasible given its maximum cruise speed V. Constraint (2f) ensures that the time it takes the searcher to travel from the entry point to the exit point of each fixed region is feasible given its on-station speed $\hat{V}$. Constraint (2g) restricts the searcher's entry point and exit point in each fixed region j to lie within the convex feasibility set $\mathcal{R}_j$. We observe that (2g) need not depend on $\boldsymbol{x}$ because $\boldsymbol{r}_j$ is a vacuous variable when region j is not searched.

3.2. Fixed Region Search Numerical Results

Returning to **BS-MS**, we include the target that exhibits large departure time uncertainty ranges, namely GF2. We assume that the fixed region entry and exit points are constrained to $\mathcal{R}_{\text{GF2}}$ the line segment between the expected departure and arrival locations of GF2; 72W 12N - 87.5W 20N. We arrive at the modified scenario **BS-FR** that now includes all four targets, but still excludes interdiction asset considerations.

The optimal solution, computed using SBB, is the same as reported in Table 2 and Figure 2. The large search area associated with GF2 results in a search value that is an order of magnitude

smaller than that of the other targets. As a result, it is not beneficial for either searcher to consume transit time in order to search for GF2.

To illustrate a search plan that includes a fixed region search in the optimal solution we consider an excursion to **BS-FR**, adjusting the intelligence data for GF2 as follows. The expected departure time is shifted 12 h earlier to 1200. The expected payload of GF is increased to 5,000 kg of drugs. Additionally, the overall certainty of the intelligence is increased to 0.95. The latter two modifications serve to increase the search value of GF2, while the first modification provides a greater opportunity for search by shifting the feasible search window of GF2 to earlier in mission execution period. We denote by **BS-FR-E** this excursion to **BS-FR** that includes these three modifications.

The optimal solution for **BS-FR-E**, computed using SBB, yields an expected search value of 2,297.0 kg of drugs detected. The optimal search plan is given in Table 3. Note that $\boldsymbol{\theta}_j^+ = \boldsymbol{r}_j^+$ and $\boldsymbol{\theta}_j^- = \boldsymbol{r}_j^-$ for $j \in R$, while $\boldsymbol{\theta}_j^+$ and $\boldsymbol{\theta}_j^-$ for $j \in Q$ represent moving search region entry and exit locations.

Searcher	Target	t	a	d	$\boldsymbol{\theta}^+$	$\boldsymbol{\theta}^-$
	Home	-	0	8.40	(89.1W 13.4N)	(89.1W 13.4N)
1	GF3	2.68	11.08	4.64	(83.9W 0.1S)	(87.7W 1.0S)
	Home	2.68	18.40	-	(89.1W 13.4N)	(89.1W 13.4N)
	Home	-	0	5.54	(89.1W 13.4N)	(89.1W 13.4N)
	GF1	1.46	7.00	0.06	(81.9W 10.0N)	(82.0W 10.0N)
2	GF1	0.00	7.06	3.13	(82.0W 10.0N)	(82.9W 12.4N)
	GF2	0.85	11.03	3.30	(80.8W 16.5N)	(86.1W 19.3N)
	Home	1.21	15.54	-	(89.1W 13.4N)	(89.1W 13.4N)

Table 3: **Restricted baseline scenario excursion BS-FR-E solution** - The plan for searcher 1 is unchanged relative to the **BS-MS** optimal solution, searcher 2 is now directed to GF2 instead of SP1.

Figure 3 depicts the optimal search plan for **BS-FR-E**. We observe that the optimal plan for searcher 1 is unchanged with respect to the optimal plan for **BS-FR**, searching for GF3 with the same search times. The optimal plan for searcher 2, however, shifts to search GF1 earlier in day 1 and then proceeds to search for GF2 in its fixed region. Recall that search is assumed to be carried out according the random search model, and the planner chooses the tactical pattern to be flown by the searchers in each search region. The large shaded search area for GF2 shown in

Figure 3 reflects the fixed geographical boundaries of the search region, and is not meant to imply that search is required be conducted everywhere in this region. In fact, searching this entire fixed region is not possible given the 3.3-h search dwell time. The GF2 search region is over 1,000 nm long ($|\bar{\boldsymbol{\rho}}_{\mathrm{GF2}} - \boldsymbol{\rho}_{\mathrm{GF2}}| = 1,014$ nm). Searcher 2 traveling at $\hat{V} = 205$ kts would take almost five hours just to transit across the region. The optimal entry and exit locations $\boldsymbol{r}^{+}_{\mathrm{GF2}}$ and $\boldsymbol{r}^{-}_{\mathrm{GF2}}$ are chosen to reduce transit time as much as possible provided that constraints (2f) and (2g) are satisfied.

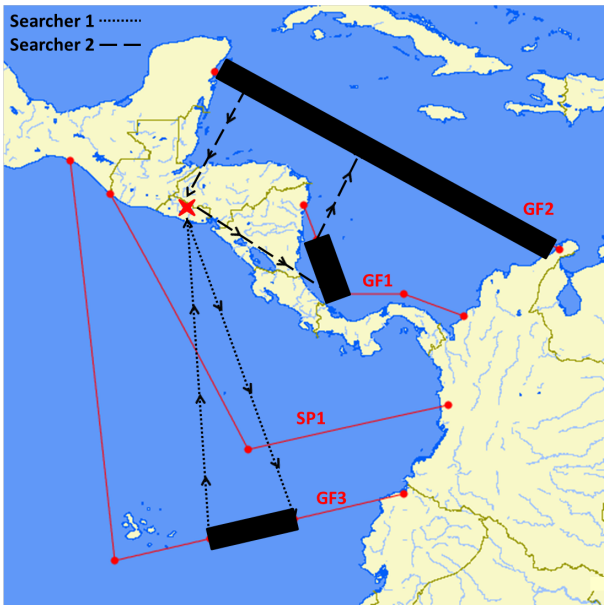

Figure 3: **Restricted baseline scenario excursion BS-FR-E solution** - Searcher 1 is routed to search GF3, while searcher 2 is routed to search GF1 and GF2. The path of searcher 2 into and out of the fixed search region for GF2 reflects the optimal values for $\boldsymbol{r}^{-}$ and $\boldsymbol{r}^{+}$ respectively. Within the search region (shaded dark) search actions are carried out according to the random search model.

4. Interdictor Positioning

4.1. Coordinated Search and Interdiction Model

We now consider search planning operations where the searcher is routed in the AOI to detect moving targets, and when a detection occurs, an interdictor is called to respond. While the interdictor is in transit to capture the detected target, the searcher monitors the target to prevent escape. At the moment the target is detected, one of three things can happen. First, the target could take evasive action by altering its intended track in an attempt to evade capture. This possibility is not considered in our one-sided search model. Search games are more appropriate models to deal with this consideration (see, e.g., Alpern and Gal 2003). Second, the target could continue on its

intended track. Third, the target could stop. The latter two possibilities can be captured by our search model by expressing the distance between the target and the interdictor using a second order cone constraint. We proceed under the assumption that targets stop when detected by a searcher.

Since the endurance of the searcher and the speed of the interdictor are both limited, we must account for the distance between the position of the interdictor and the location where a detection may occur. The interdictor may be positioned at a given location that cannot be changed by the mission planner. In this case, the feasible search area is constrained by the interdictor's location. Alternatively, the standby location of the interdictor may be a decision variable. Yet another possibility exists where the search controller may specify an initial standby position for the interdictor, as well as a drift course and speed (*drift vector*). We model the latter as it is the more general case.

Let $\boldsymbol{p} \in \mathcal{P}$ be the initial standby position of the surface interdictor, where $\mathcal{P}$ is a convex set. Let $\hat{\boldsymbol{p}} \in \mathcal{P}$ be the final position of the surface interdictor at the end of the mission execution period. Let $\boldsymbol{v}$ be the drift vector of the surface interdictor. Let V_I be the intercept speed of the interdictor. We assume that if a detection occurs in any searched region, the searcher will stay on station as required so that the interdictor may respond. Therefore, the interdictor must be able to travel to the search region before the mission execution period expires and before the searcher reaches its endurance limit. In the unlikely event that multiple detections occur at the same time for the same interdictor, we assume that the interdictor will respond to the first call it receives from a searcher. We also assume that the searcher maintains a safety stock of fuel so that, when it has to monitor a detected target, it is still able to return to home station at the end of its mission. We account for safety stock through *backtracking time* b_j, which is the minimum time required for the searcher to return to home station from any point on target segment j that is assigned to be searched. Backtracking time can be modeled as a fixed value, possibly different for each target, or as a decision variable. We choose the latter as it is the more general case. The interdictor coordinated SSP is stated as follows.

Problem SSP-I:

$$\max_{\boldsymbol{a},\boldsymbol{d},\boldsymbol{t},\boldsymbol{b},\boldsymbol{p},\hat{\boldsymbol{p}},\boldsymbol{x},\boldsymbol{y}} \quad \sum_{j\in N} q_j \left(1-\exp\left\{-\alpha_j d_j y_j\right\}\right) \tag{3a}$$

$$\text{s.t.} \quad (||\boldsymbol{\rho}_i + (a_i - \tau_i)\boldsymbol{u}_i - \boldsymbol{p} - a_i\boldsymbol{v}|| \\ \ldots - V_I(T + d_0 - b_i - a_i))y_i \leq 0, \quad \forall i \in \hat{N} \tag{3b}$$

$$(||\boldsymbol{\rho}_i + (a_i + d_i - \tau_i)\boldsymbol{u}_i - \boldsymbol{p} - (a_i + d_i)\boldsymbol{v}|| \\ \ldots - V_I(T + d_0 - b_i - a_i - d_i))y_i \leq 0, \quad \forall i \in \hat{N} \tag{3c}$$

$$(||\boldsymbol{\rho}_i + (a_i - \tau_i)\boldsymbol{u}_i - \boldsymbol{p} - a_i\boldsymbol{v}|| \\ \ldots - V_I(D - b_i - a_i))y_i \leq 0, \quad \forall i \in \hat{N} \tag{3d}$$

$$(||\boldsymbol{\rho}_i + (a_i + d_i - \tau_i)\boldsymbol{u}_i - \boldsymbol{p} - (a_i + d_i)\boldsymbol{v}|| \\ \ldots - V_I(D - b_i - a_i - d_i))y_i \leq 0, \quad \forall i \in \hat{N} \tag{3e}$$

$$(||\boldsymbol{\rho}_i + (a_i - \tau_i)\boldsymbol{u}_i - \boldsymbol{\rho}_{n+1}|| - Vb_i)y_i \leq 0, \quad \forall i \in \hat{N} \tag{3f}$$

$$(||\boldsymbol{\rho}_i + (a_i + d_i - \tau_i)\boldsymbol{u}_i - \boldsymbol{\rho}_{n+1}|| - Vb_i)y_i \leq 0, \quad \forall i \in \hat{N} \tag{3g}$$

$$\boldsymbol{p} + a_{n+1}\boldsymbol{v} - \hat{\boldsymbol{p}} = \boldsymbol{0} \tag{3h}$$

$$\boldsymbol{p}, \hat{\boldsymbol{p}} \in \mathcal{P} \tag{3i}$$

$$\text{(1b) – (1m)}$$

Constraints (3b) and (3c) require that the distance between where search occurs and position of interdictor is within the travel range of the searcher given the amount of time remaining relative to the endurance limit of the searcher. Figures 4 and 5 illustrate how constraints (3b) and (3c) function in this model. We assume a negligible proportion of the search region falls outside of the interdictor response circle, and that the maximum speed of the interdictor is faster than its intercept speed. This allows the interdictor to successfully respond when the searcher detects a target within its search region and just outside of the interdictor response range. Similarly, constraints (3d) and (3e) require that the distance between where search occurs and position of interdictor is within the travel range of the searcher given the amount of time remaining in the planning cycle. Constraints (3f) and (3g) require that the distance between where search occurs and searcher's home station is within the backtracking time travel range of the searcher. Constraint (3h) sets the final resting position of the interdictor to be its drifted position at the moment the searcher returns to home

station. Constraint (3i) requires that the position of the interdictor remain within the feasibility set $\mathcal{P}$ throughout the mission.

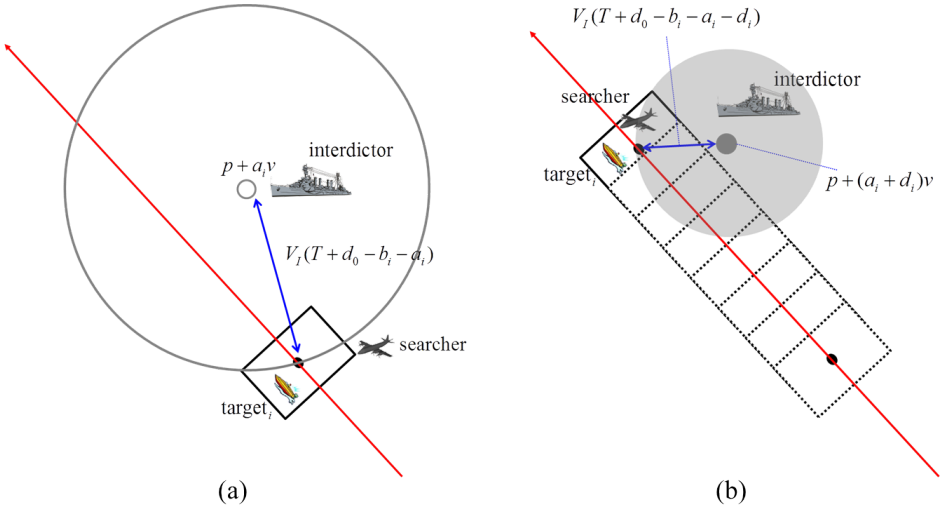

Figure 4: **Interdiction model diagram** - Consider a straight line movement track for target i and rectangular search region as shown. (a) Constraint (3b) requires that the distance between where search begins against target i and the position of the interdictor at the time search commences $\boldsymbol{p}+a_i\boldsymbol{v}$ is no greater than the range of the interdictor $V_I(T + d_0 - b_i - a_i)$. The search region at the moment search begins against target i is shown as the solid rectangle. The interdictor response circle with radius $V_I(T + d_0 - b_i - a_i)$ and center $\boldsymbol{p} + a_i\boldsymbol{v}$ is shown. (b) Constraint (3c) requires that the distance between where search ends against target i and the drifted position $\boldsymbol{p} + (a_i + d_i)\boldsymbol{v}$ of the interdictor is no greater than the range of the interdictor $V_I(T + d_0 - b_i - a_i - d_i)$. The search region at the moment search ends against target i is shown as the solid rectangle. The search region moving over time epochs is shown as indicated by the dotted rectangles. The interdictor response circle with radius $V_I(T + d_0 - b_i - a_i - d_i)$ and center $\boldsymbol{p} + (a_i + d_i)v$ are shown.

The special case where the position of the interdictor is fixed and unchangeable can be modeled by fixing $\boldsymbol{p}$ and $\boldsymbol{v} = \boldsymbol{0}$. Similarly, other situations can be modeled by allowing $\boldsymbol{p}$ to vary and/or choosing $\boldsymbol{v} \neq \boldsymbol{0}$. Multiple interdictors are easily handled with this model by indexing the variables and parameters associated with the interdictor. If each target can be matched to an interdictor, the multiple interdictor model is no more difficult to solve than the single interdictor model. When the target-to-interdictor matching is unknown or cannot reasonably be set manually, this introduces integer variables that must be handled along with $\boldsymbol{x}$ through branching. Since predetermined patrol zones and state sovereignty may often drive surface interdictor placement, we assume that the target-to-interdictor matching can be done manually.

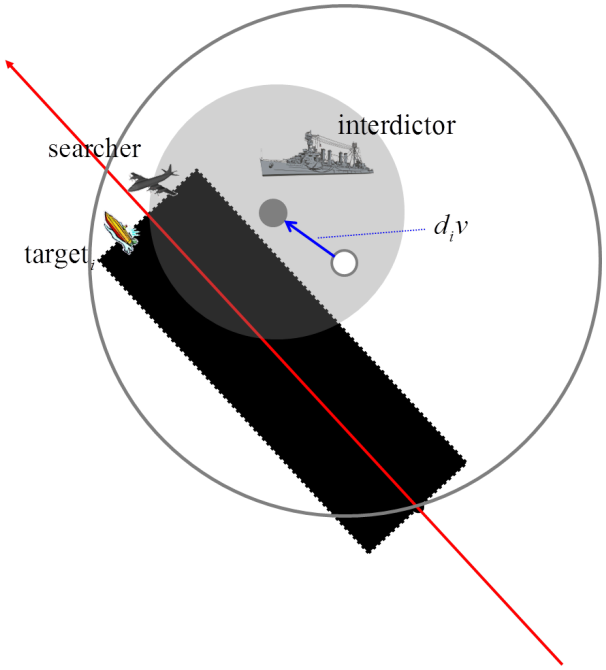

Figure 5: **Interdiction model diagram combined** - We combine both parts of Figure 4 by shading the response circle associated with constraint (3c) and filling in the moving search region as done in previous illustrations. Interdiction model solution figures later in this section will have this representation. We see that the center of the shaded response circle is offset by the vector $d_i \boldsymbol{v}$. We observe that when $\boldsymbol{v} = \boldsymbol{0}$, the centers of the response circles must be the same position $\boldsymbol{p}$.

4.2. Coordinated Search and Interdiction Numerical Results

Returning to **BS** we assume that interdictors are assigned in regional zones as indicated in Table 4. Recall that the intercept speed of the interdictor is $V_I = 20$ kts.

Interdictor	Targets	Zone
1	GF1, GF2	SW Caribbean zone
2	GF4, SP1, SP3	NE Eastern Pacific zone
3	GF3	SW Eastern Pacific zone

Table 4: **Zonal interdictor-to-target assignment for scenario BS**

We augment the restricted scenario **BS-FR** by including interdiction assets. We assume that backtracking time for each searcher is included in its endurance time T; we fix $b_j = 0, \forall j \in N$, and we relax backtracking time constraints (3f) and (3g). In keeping with **BS** in Section 2, we do not allow the interdictors to change position after their location has been coordinated with the search plan. Therefore, we require $\boldsymbol{v} = \mathbf{0}$ and $\boldsymbol{p} = \hat{\boldsymbol{p}}$. We restrict the positions of interdictor 1 to be within the Caribbean Sea, and the positions of interdictors 2 and 3 to be within the eastern Pacific Ocean. Accordingly, feasible polyhedral sets $\mathcal{P}_k$ for interdictors $k = 1, 2, 3$ are defined by the convex hulls of the sets of extreme points given in Table 5 and the polyhedral sets are depicted in Figure 6.

Interdictor (k)	Extreme Points of $\mathcal{P}_k$
1	(70W 25N), (90W 22N), (82W 10N), (76.3W 9N), (72W 12N)
2	(100W 5S), (81W 5S), (77W 6N), (100W 17N)
3	(100W 5S), (81W 5S), (77W 6N), (100W 17N)

Table 5: **Interdictor position polyhedral sets extreme points**

Scenario **BS** is solved using SBB, yielding an expected search plan value of 2,189.8 kg of drugs detected. The optimal search plan and interdictor placements are reported in Table 6 and Table 7. The optimal search plan differs from the optimal search plan for **BS-FR** reported in Table 2 in how the search effort for GF3 is allocated. In **BS**, while it is optimal to search GF3, the search happens farther to the east and it is searched for a shorter period of time due to the restricted range of the interdictor.

Figure 7 shows a spatial representation of the optimal search plan. As the interdictor response circles indicate, the search plan relative to GF1 and SP1 are not limited by the range of the

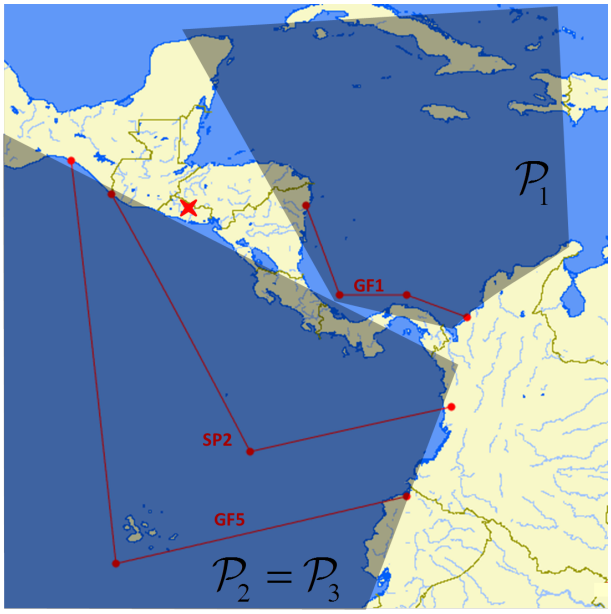

Figure 6: **Feasible interdictor position polyhedral sets** - Interdictor 1 can be positioned anywhere in $\mathcal{P}_1$. Interdictors 2 and 3 can be positioned anywhere in $\mathcal{P}_2$, which is the same as $\mathcal{P}_3$.

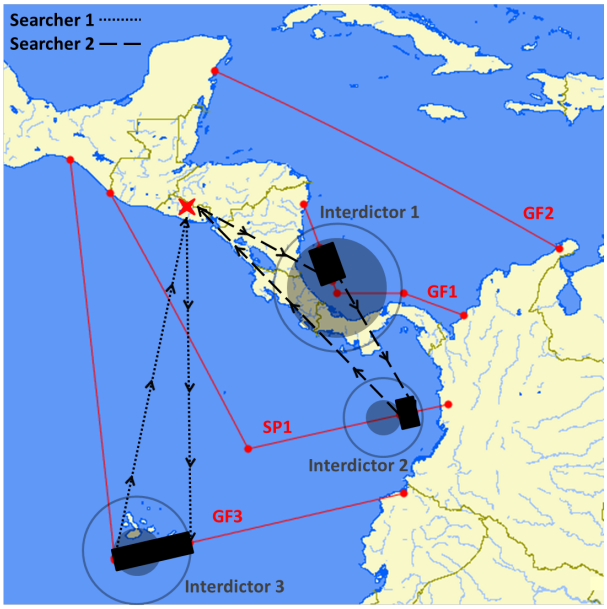

Figure 7: **Scenario BS optimal solution** - The resulting expected value of the search plan is 2,189.8 kg of drugs detected, which is less than the expected search plan value associated with **BS-FR** due to the restrictions induced by the interdictor ranges. The size of the rectangular blocks correspond to the total area of the search region during the time when the searcher is performing search actions. The large transparent outlined outer circles, with optimal interdictor standby locations at the center, represent the response range, based on constraints (3b), of each respective interdictor at the moment search begins for its assigned target. The small shaded inner circles, again with optimal interdictor standby locations at the center, represent the response range, based on constraints (3c), of each respective interdictor at the moment search ends for its assigned target.

Searcher	Target	t	a	d	$\boldsymbol{\theta}^+$	$\boldsymbol{\theta}^-$
1	Home	-	0	14.16	(89.1W 13.4N)	(89.1W 13.4N)
	GF3	2.71	16.87	4.24	(88.6W 1.2S)	(92.0W 1.9S)
	Home	2.89	24.00	-	(89.1W 13.4N)	(89.1W 13.4N)
2	Home	-	0	6.39	(89.1W 13.4N)	(89.1W 13.4N)
	GF1	1.37	7.76	1.91	(82.2W 10.6N)	(82.8W 12.0N)
	SP1	1.57	11.24	2.69	(78.5W 4.7N)	(79.2W 4.5N)
	Home	2.46	16.39	-	(89.1W 13.4N)	(89.1W 13.4N)

Table 6: **Optimal search times and searcher path for scenario BS** - Expected value of the optimal search plan is 2,189.8 kg of drugs detected.

Interdictor	Position
1	(81.9W 10N)
2	(79.9W 4.1N)
3	(91.0W 1.7S)

Table 7: **Optimal interdictor standby positions for scenario BS**

interdictor. The GF1-interdictor 1 range circles could be shifted in the northwest direction and the search plan would still be feasible. Similarly, the SP1-interdictor 2 range circles could be shifted east. This is not the case for the GF3-interdictor 3 range circles. The edge of the outer interdictor range circle is tangent to the point $\boldsymbol{\theta}^+_{\text{GF3}}$ where search begins against GF3, while the edge of the inner interdictor range circle is tangent to the point $\boldsymbol{\theta}^-_{\text{GF3}}$ where search ends against GF3. This indicates that the search plan relative to GF3 is limited by the range of the interdictor, and it highlights why the optimal search plan for **BS** differs from that of **BS-FR**.

As an alternative, one might consider using the optimal solution for **BS-FR** and simply adding in the interdictor position later by solving a single nonlinear program with decision variable vector $\boldsymbol{p}$ (e.g., solve **SSP-I** by fixing all variables except $\boldsymbol{p}$). Such a strategy may appear practical in situations where interdictor coordination is an afterthought, an optimal solution to **SSP-FR** is already in hand, and there is not enough time to set-up and solve **SSP-I**. Unfortunately this approach does not work in general, because there is no guarantee that the incumbent search plan is feasible with respect to interdictor ranges. Taking the optimal search plan solution to **BS-FR** and overlaying the interdictor response circles we arrive at Figure 8. Given 4.64 h of search dwell

time against GF3, there is no point $\boldsymbol{p}$ that can satisfy both constraint (3b) and constraint (3c) for interdictor 3 and GF3. The situation depicted illustrates that when the point $\boldsymbol{\theta}^{+}_{\text{GF3}}$ where search begins is contained in the outer circle, the point $\boldsymbol{\theta}^{-}_{\text{GF3}}$ where search ends cannot be contained in the inner circle.

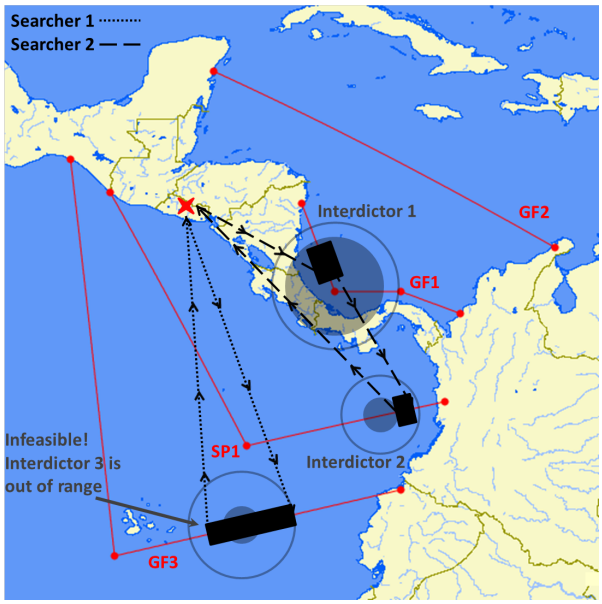

Figure 8: **Interdictor infeasibility of the restricted baseline scenario BS-FR solution** - The search boxes depicted represent the optimal search plan for **BS-FR**. The large transparent outlined outer circles represent the response range based on constraints (3b). The small shaded inner circles represent the response range based on constraints (3c). Given 4.64 h of search dwell time against GF3, there is no point $\boldsymbol{p}$ that can satisfy both of these constraints for interdictor 3 and GF3. The situation depicted here shows that when the point $\boldsymbol{\theta}^{+}_{\text{GF3}}$ where search begins is contained in the outer ring, the point $\boldsymbol{\theta}^{-}_{\text{GF3}}$ where search ends cannot be contained in the inner ring.

Another alternative that one might consider is to use the optimal searcher path $\boldsymbol{x}^{*}$ for **BS-FR** and solving a single NLP for all continuous variables in **SSP-I**. Such a strategy is also not guaranteed to yield a feasible solution. This is easily seen in a situation where at least two searched targets in the same interdiction zone are too far apart. In such a situation there would be no interdictor position $\boldsymbol{p}$ that could support searching both targets. In **BS-FR**, however, since no more than one target in each interdiction zone is searched in the optimal plan, we can obtain an interdictor-feasible plan using this strategy. This approach results in the search plan and interdictor placement given in Tables 8 and 9 respectively. This strategy produces a suboptimal plan, albeit by a small margin, with an expected search value that is 2.1 kg less than the optimal plan (given in Tables 6 and 7). While the optimality gap in this case is small, we note that its magnitude is entirely driven by the expected payload of GF3. This gap will grow proportionally to the expected payload of GF3.

Figure 9 shows a spatial representation of this suboptimal search plan. We observe that the search region for GF3 in this plan is shifted to the northeast and is slightly smaller than the search region for GF3 Figure 7.

Searcher	Target	t	a	d	$\boldsymbol{\theta}^+$	$\boldsymbol{\theta}^-$
1	Home	-	0	10.75	(89.1W 13.4N)	(89.1W 13.4N)
	GF3	2.66	13.40	4.20	(85.8W 0.6S)	(89.2W 1.4S)
	Home	2.73	20.33	-	(89.1W 13.4N)	(89.1W 13.4N)
2	Home	-	0	6.39	(89.1W 13.4N)	(89.1W 13.4N)
	GF1	1.37	7.76	1.91	(82.2W 10.6N)	(82.8W 12.0N)
	SP1	1.57	11.24	2.69	(78.5W 4.7N)	(79.2W 4.5N)
	Home	2.46	16.39	-	(89.1W 13.4N)	(89.1W 13.4N)

Table 8: **Optimal search times and searcher path using the optimal searcher path $\boldsymbol{x}$ for BS-FR** - Expected value of the search plan is 2,187.8 kg of drugs detected.

Interdictor	Position
1	(82W 10N)
2	(79.9W 4.1N)
3	(88.2W 1.1S)

Table 9: **Interdictor standby positions using the optimal searcher path $\boldsymbol{x}^*$ for BS-FR**

5. Conclusions

This article improves existing search modeling capability by introducing two important model extensions. We define a fixed region search model that gives mission planners the ability to account for situations where assessed target data is highly uncertain. We also introduce a coordinated search and interdiction model that is able to directly model the interaction of aerial searchers and surface interdictors. This important model eliminates troublesome situations where smugglers are detected, but they get away because there are no interdictors nearby to intercept them.

We demonstrate how these models can be used through a benchmark scenario that was developed by researchers and practitioners so that it is representative of the real-world issues faced by planners. We investigate the impact of not coordinating search with interdiction assets and show that this can result in suboptimal or infeasible search plans.

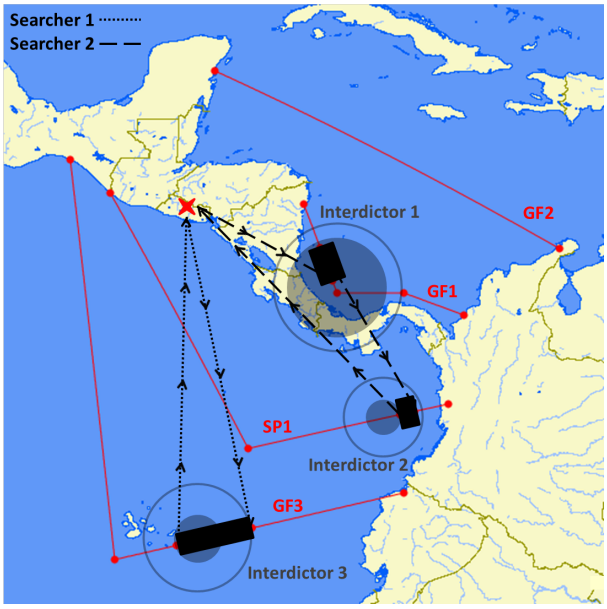

Figure 9: **Suboptimality of the restricted baseline scenario BS-FR fixed search order when adding interdictors** - The search boxes depicted represent the optimal search times for the **BS-FR** fixed search order. The large transparent outlined outer circles represent the response range based on constraints (3b). The small shaded inner circles represent the response range based on constraints (3c). Adding interdictor coordination to the fixed search order for **BS-FR** yields a plan whose objective function is 2.1 kg less than the optimal plan. This because the interdictor range restriction drives a slightly smaller search region for GF3.

Acknowledgement

The second author acknowledges financial support from the Office of Naval Research, Mathematical Optimization and Operations Research Program.

References

Alpern, S., Gal, S., 2003. The Theory of Search Games and Rendezvous. International Series in Operations Research & Management Science. Kluwer, New York, NY.

Benkoski, S., Monticino, M., Weisinger, J., 1991. A Survey of Search Theory Literature. Naval Research Logistics 38, 469–494.

Dell, R., Eagle, J., Martins, G., Santos, A., 1996. Using Multiple Searchers in Constrained-Path, Moving-Target Search Problems. Naval Research Logistics 43 (4), 463–480.

Eagle, J., Yee, J., 1990. An optimal branch-and-bound procedure for the constrained path, moving target search problem. Operations Research 38 (1), 110–114.

Grundel, D., 2005. Constrained search for a moving target. In: Proceedings of the 2005 international conference on Collaborative technologies and systems. CTS'05. IEEE Computer Society, Washington, DC, St. Louis, MO, pp. 327–332.

Jin, Y., Liao, Y., Minai, A. A., Polycarpou, M. M., 2006. Balancing search and target response in cooperative unmanned aerial vehicle (UAV) teams. IEEE transactions on systems man and cybernetics Part B Cybernetics a publication of the IEEE Systems Man and Cybernetics Society 36 (3), 571–587.

Joint Interagency Task Force South, 2014. Serving the nation for over 20 years. Retrieved June 3, 2014, http://www.jiatfs.southcom.mil/index.aspx.

Kress, M., Royset, J. O., Rozen, N., 2012. The eye and the fist: Optimizing search and interdiction. European Journal of Operational Research 220 (2), 550–558.

Munsing, E., Lamb, C. J., 2011. Joint Interagency Task Force-South: The Best Known, Least Understood Interagency Success. Strategic Perspectives. National Defense University Press, Washington, D.C.

Pietz, J., Royset, J. O., 2013. Generalized Orienteering Problem with Resource Dependent Rewards. Naval Research Logistics 60 (4), 294–312.

Riehl, J. R., Collins, G. E., Hespanha, J. P., 2007. Cooperative graph-based model predictive search. 2007 46th IEEE Conference on Decision and Control (i), 2998–3004.

Royset, J. O., Sato, H., 2010. Route Optimization for Multiple Searchers. Naval Research Logistics 57 (8), 701–717.

Sato, H., Royset, J. O., 2010. Path Optimization for the Resource-Constrained Searcher. Naval Research Logistics 57 (5), 422–440.

Stewart, T., 1979. Search for a moving target when searcher motion is restricted. Computers and Operations Research 6, 129–140.

Sun, A. K., 2009. Cooperative UAV Search and Intercept. Master's thesis, University of Toronto, Toronto, ON, Canada.

Trummel, K., Weisinger, J., 1986. The Complexity of the Optimal Searcher Path Problem. Operations Research 34 (2), 324–327.

United Nations Office on Drugs and Crime, 2012. World Drug Report. United Nations, New York, NY.

US Department of Justice, 2014. National Drug Threat Assessment. Retrieved June 3, 2014, http://www.justice.gov/archive/ndic/pubs38/38661/movement.htm.

Washburn, A. R., 2002. Search and Detection, 4th Edition. INFORMS, Linthicum, Maryland.

Wong, E., Bourgault, F., Furukawa, T., 2005. Multi-vehicle Bayesian search for multiple lost targets. In: Proceedings of the 2005 IEEE Internationl Conference on Robotics and Automation. Barcelona, Spain, pp. 3169–3174.